Relativistic *ab initio* description of the *K*-vacancy production in heavy-ion–atom collision systems with solid targets

P. Kürpick, W.-D. Sepp, and B. Fricke
Fachbereich Physik, Universität Kassel, 34109 Kassel, Germany
(Received 25 July 1994)

We investigate the problem of ion–solid-target collisions by means of a time-dependent coupled-channel description using *ab initio* relativistic four-component linear-combination-of-atomic-orbital molecular-orbital (LCAO-MO) wave functions as a basis. Large-impact-parameter calculations allow us to determine how the *L* and *M* shells of initially low ionized projectiles are fully stripped within a few atomic layers of the solid target. Once the inner-*L*-shell vacancies are created, our narrow-impact-parameter calculations give very good agreement with experimental results on *K*-shell vacancy production. As an example, we compare our results with measurements of 40.6-MeV Ar^{4+} and Ar^{12+} ions on Ca solid targets.

PACS number(s): 34.10.+x, 31.15.−p

I. INTRODUCTION

The mechanism of electronic *K*-*L* shell charge transfer processes in slow ion-atom collisions is well understood within the molecular-orbital model: The $2p\pi$-$2p\sigma$ rotational coupling and the $2p\sigma$-$1s\sigma$ radial coupling are the dominant dynamical coupling matrix elements which explain the charge transfer from an empty atomic *L* shell to the *K* shell of the target atom [1]. Beyond this qualitative explanation the goal still remains to give a quantitative description of such a collision, especially for heavy relativistic collision systems where the initial vacancies are not in the *L* shell but in the higher *M* shell. One attempt to calculate *L*-shell ionization probabilities in low-energy heavy collision systems was performed by Schulze [2] using a variable screening model with relativistic corrections from Eichler and Wille [3]. To describe the complete collision with the transfer of high-lying vacancies into the *K* shell after the collision we perform time-dependent many-electron coupled-channel calculations using molecular relativistic linear-combination-of-atomic-orbital molecular-orbital (LCAO-MO) Dirac-Fock-Slater basis functions. All dynamic coupling matrix elements are also calculated in an *ab initio* way. In this paper we give a brief outline of the method, especially the calculation of the dynamic coupling matrix element, and compare our results as an example with solid target measurements for the *K*-shell vacancy production in collisions of 40.6-MeV Ar ions on Ca performed by Kambara *et al.* [4].

II. METHOD

Ab initio self-consistent LCAO-MO Dirac-Fock-Slater molecular orbitals form a basis which allow a very good description of low- and medium-energy ion-atom collisions [5–9]. The most recent method is described here in brief.

We start from the time-dependent Dirac-Fock-Slater (TDDFS) equation

$$\left[\hat{t}+\hat{V}^{N}(t)+\hat{V}^{C}(t)+\hat{V}_{\alpha}^{\mathrm{ex}}(t)-i\hbar\frac{\partial}{\partial t}\right]\psi_i(t) = \left[\hat{h}^{\mathrm{TDDFS}}(t)-i\hbar\frac{\partial}{\partial t}\right]\psi_i(t)=0\ ,\quad i=1,\ldots,N\ ,$$

which is obtained from the variation of the functional

$$I=\int_{-\infty}^{+\infty}dt\left\langle\Psi\left|H-i\hbar\frac{\partial}{\partial t}\right|\Psi\right\rangle\ ,\quad \Psi=\det(\psi_1,\ldots,\psi_N)\ .$$

$V^{N}(t)$ is the electron-nuclear potential, $V^{C}(t)$ is the Coulomb potential, and $V_{\alpha}^{Ex}(t)$ is the Slater exchange potential. In our ansatz the time-dependent wave function $\psi_i(\vec{r},t)$ is expanded in a set of self-consistent single-particle molecular wave functions,

$$\psi_i(\vec{r},t)=\sum_{j}^{M}a_{ij}(t)\phi_j(\vec{r};\vec{R}(t))\ . \tag{1}$$

In the adiabatic regime we neglect small-potential coupling terms [10] and the basis-set expansion (1) leads to a set of equivalent first-order differential equations

$$\dot{a}_{ij}=\sum_{j}-a_{im}\left\langle\phi_j\left|\frac{\partial}{\partial t}\right|\phi_m\right\rangle e^{-(i/\hbar)\int(\varepsilon_m-\varepsilon_j)dt'} \tag{2}$$

for the time-dependent single-particle amplitudes a_{ij}. To calculate many-particle probabilities in the scheme of inclusive probabilities [11] we need to evaluate the single-particle density matrix and therefore have to solve the coupled equation (2) for all the *N* initial conditions,

$$\lim_{t\to-\infty}[\psi_i(t)-\psi_i^{0}(t)]=0\ ,\quad i=1,\ldots,N\ .$$

$\psi_i^{0}(t)$ is the initially occupied atomic orbital to which the molecular orbital $\psi_i(t)$ tends for $t=-\infty$.

The molecular basis functions ϕ_j are chosen to be eigenfunctions of the time-independent Dirac-Fock-Slater equation

$$\hat{h}^{\mathrm{MO}}(\vec{R})\phi_j(\vec{r};\vec{R})=[\hat{t}+\hat{V}^N(\vec{R})+\hat{V}^C(\vec{R})+\hat{V}^{\mathrm{ex}}_\alpha(\vec{R})]\phi_j(\vec{r};\vec{R})$$
$$=\varepsilon_j(\vec{R})\phi_j(\vec{r};\vec{R})\ . \tag{3}$$

The solution of Eq. (3) is achieved by expanding the molecular wave functions ϕ_j in numerically given atomic four-component Dirac spinors,

$$\phi_j(\vec{r};\vec{R})=\sum_{\nu=1}^{S} c_{j\nu}(\vec{R})\xi_\nu(\vec{r};\vec{R})\ ,$$
$$\langle\vec{r}|\xi_\nu(\vec{R})\rangle\equiv\xi_{n\kappa m_j}(r,\Omega)$$
$$=\frac{1}{r}\begin{bmatrix} G_{n\kappa}(r)\mathcal{Y}_{+\kappa,m_j}(\Omega) \\ iF_{n\kappa}(r)\mathcal{Y}_{-\kappa,m_j}(\Omega)\end{bmatrix},$$

which can be located anywhere on the internuclear axis. $G_{n\kappa}$ and $F_{n\kappa}$ are the great and small components of the Dirac spinor while $\mathcal{Y}_{+\kappa,m_j}$ is the spherical harmonic.

The static Dirac-Fock-Slater equation (3) is therefore reduced to the secular equation

$$\mathbf{h}^{\mathrm{MO}}\mathbf{c}=\varepsilon\mathbf{S}\mathbf{c} \tag{4}$$

which has to be solved self-consistently for a large number of internuclear distances. Typically we solve Eq. (4) at about 100 internuclear distances to get both accurate eigenvalues and matrix elements along the whole trajectory.

The molecular-dynamic coupling-matrix (CM) element

$$\left\langle\phi_l\left|\frac{\partial}{\partial t}\right|\phi_m\right\rangle+\dot{R}\left\langle\phi_l\left|\frac{\partial}{\partial R}\right|\phi_m\right\rangle-\frac{i\dot{\theta}}{\hbar}\langle\phi_l|j_y^{\mathrm{CM}}|\phi_m\rangle$$

is reduced by means of the atomic basis-set representation of the molecular orbitals to four matrix elements involving only one- and two-center atomic matrix elements,

$$\left\langle\phi_l\left|\frac{\partial}{\partial t}\right|\phi_m\right\rangle=\dot{R}\sum_{\nu,\mu}c_{l\nu}^*\left[\frac{\partial}{\partial R}c_{m\mu}\right]\langle\xi_\nu|\xi_\mu\rangle+\dot{R}\sum_{\nu,\mu}c_{l\nu}^*c_{m\mu}\left\langle\xi_\nu\left|\frac{\partial}{\partial R}\right|\xi_\mu\right\rangle$$
$$-\frac{i\dot{\theta}}{\hbar}\sum_{\nu,\mu}c_{l\nu}^*c_{m\mu}\langle\xi_\nu|j_y^K|\xi_\mu\rangle+\frac{i\dot{\theta}}{\hbar}\sum_{\nu,\mu}c_{l\nu}^*c_{m\mu}R_K\langle\xi_\nu|p_x|\xi_\mu\rangle$$
$$=M^{\mathrm{MO}}+M^{\mathrm{kinetic}}-M^{\mathrm{orientation}}+M^{\mathrm{displacement}}\ . \tag{5}$$

The latter two orientation and displacement parts of the rotational coupling are generated through the decomposition of the angular momentum operator (see Fig. 1).

$$j_y^{\mathrm{CM}}=\vec{l}+\vec{s}=(\vec{r}_i\times\vec{p})+\vec{s}=[(\vec{R}_K+\vec{r}_i^{\,K})\times\vec{p}\,]+\vec{s}$$
$$=j_y^K+[\vec{R}_K\times\vec{p}\,]_y$$

with

$$\vec{R}_k=(\pm)\frac{M_K}{M_P+M_T}\vec{R}\ .$$

K denotes the projectile (target) nucleus where the corresponding atomic orbital is centered.

By using the definition of the momentum operator the displacement part of the radial coupling-matrix element can further be reduced to

$$M^{\mathrm{kinetic}}=\dot{R}\sum_{\nu,\mu}c_{l\nu}^*c_{m\mu}\left\langle\xi_\nu\left|\frac{\partial}{\partial R}\right|\xi_\mu\right\rangle$$
$$=\dot{R}\sum_{\nu,\mu}c_{l\nu}^*c_{m\mu}\frac{M_K}{M_P+M_T}\frac{i}{\hbar}\langle\xi_\nu|p_z|\xi_\mu\rangle\ .$$

M_T (M_P) denotes the target (projectile) nucleus mass, while M_K denotes the target or projectile mass depending on where the orbital ξ_μ is centered.

By insertion of a complete set of atomic orbitals we can further reduce the orientation part of the rotational coupling-matrix element to a one-center angular momentum operator and a one-center (two-center) atomic overlap integral,

$$M^{\mathrm{orientation}}=\frac{i\dot{\theta}}{\hbar}\sum_{\nu,\mu}c_{l\nu}^*c_{m\mu}\langle\xi_\nu^{K(\nu)}|j_y^K|\xi_\mu^{K(\mu)}\rangle$$
$$=\frac{i\dot{\theta}}{\hbar}\sum_{\nu,\mu}c_{l\nu}^*c_{m\mu}\sum_\lambda\langle\xi_\nu^{K(\nu)}|\xi_\lambda^{K(\lambda)}\rangle$$
$$\times\langle\xi_\lambda^{(\lambda)}|j_y^K|\xi_\mu^{K(\mu)}\rangle\ .$$

$K(\nu)$ and $K(\mu)$ $[K(\lambda)=1,2]$ denote the projectile (target) nucleus depending on where the orbitals ξ_ν, ξ_μ, or ξ_λ are centered.

The molecular part of the radial coupling-matrix element contains explicitly the first derivative of the coefficients $c_{j\nu}$ with respect to the internuclear coordinate

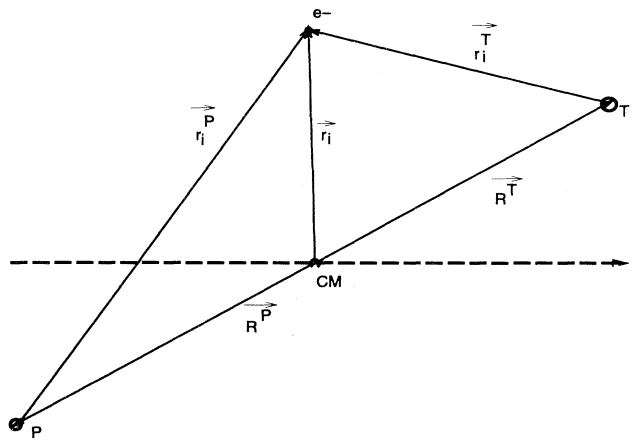

FIG. 1. Center-of-mass (c.m.) coordinate system.

R. We calculate $\partial c_{j\nu}/\partial R$ using a three-point-formula and therefore additionally have to solve the full secular equation (3) at internuclear distances $R \pm \Delta R$. Typically we set $\Delta R = 10^{-5}$ a.u. in our calculations. The molecular wave functions being eigenfunctions of m_j, M^{MO} obeys the selection rule $\Delta m_j = 0$.

Using the well-known raising and lowering operators

$$j_+ = j_x + ij_y \ ,$$

$$j_- = j_x - ij_y \ ,$$

with

$$j_+ |j,m\rangle = \sqrt{(j+m+1)(j-m)}\hbar |j,m+1\rangle \ ,$$

$$j_- |j,m\rangle = \sqrt{(j-m+1)(j+m)}\hbar |j,m-1\rangle \ ,$$

the angular moment part of $M^{\mathrm{orientation}}$ can be calculated analytically. $M^{\mathrm{orientation}}$ obeys the selection rule $\Delta m_j = \pm 1$.

Finally, we use the identities

$$\hat{p}_x = \tfrac{1}{2}[\hat{\alpha}_x(\hat{\alpha}\hat{p}) + (\hat{\alpha}\hat{p})\hat{\alpha}_x] \ ,$$

$$\hat{p}_z = \tfrac{1}{2}[\hat{\alpha}_z(\hat{\alpha}\hat{p}) + (\hat{\alpha}\hat{p})\hat{\alpha}_z]$$

to evaluate M^{kinetic} and $M^{\mathrm{displacement}}$. For details on the integration rule, orthogonalization, and diagonalization procedure we refer the reader to the paper of Sepp *et al.* [5].

Until now in our calculations we have not taken into account explicit translation factors. Nevertheless, the kinetic part of the radial coupling-matrix element and the displacement part of the rotational coupling-matrix element would at least asymptotically be canceled by atomic translation factors [12]. We therefore in the close-coupling equation set M^{kinetic} and $M^{\mathrm{displacement}}$ to zero, knowing that for small internuclear distances the molecular picture would demand a switching function. Neglecting M^{kinetic} and $M^{\mathrm{displacement}}$ therefore corresponds to an implicit accounting of atomic translation factors along the whole trajectory.

The classical trajectories of the nuclei can be deduced either by using a model potential like the Coulomb potential or the screened Bohr potential or by the fully self-consistent interatomic potential which we gain from solving Eq. (4). After solving the matrix equation (2) for $-\infty \leq t \leq +\infty$ the formalism of inclusive probabilities allows us to calculate many-particle probabilities from the time-dependent single-particle amplitudes a_{ij} [11,13–19].

III. RESULTS AND DISCUSSION

In this paper we focus on the collision system 40.6-MeV Ar^{4+} or Ar^{12+} on Ca where experimental results on *K-L* vacancy sharing from Kambara *et al.* [4] are available. The measurements were done using a solid Ca target of variable thickness from 2 μg/cm^2 up to 30 μg/cm^2. Both the vacancy production in the Ar *K* shell and the Ca *K* shell were measured. Up to 8-μg/cm^2 target thickness the experimental results for the impact-parameter-dependent P_K vacancy production do not differ much and show a maximum at $b = 2500$ fm. Only the 30-μg/cm^2 Ca target gives significantly enhanced P_K vacancy probabilities both for Ca and Ar and a shift of the maximum towards smaller impact parameters, which was presumed by Kambara *et al.* as due to multiple scattering processes. The measurements were done both for Ar^{4+} and Ar^{12+} projectiles showing no significant difference in the *K*-vacancy production.

To describe the collision system we use a basis set of 38 molecular wave functions. Each molecular wave function is a linear combination of four-component Dirac spinors, namely, the $1s_{1/2}$ to $3p_{3/2}$ atomic oribtals at the Ar site and the $1s_{1/2}$ to $4s_{1/2}$ atomic orbitals at the Ca site. The smallest impact parameter measured experimentally is about 500 fm. At this smallest internuclear distance target and projectile *K* shells are not strongly overlapping. Our experience shows that the minimal basis set buildup by the separated atom orbitals is accurate enough to describe the system because the united atom behavior of the collision system is not yet predominant.

Figure 2 shows the correlation diagram which results from our self-consistent-field molecular-orbital (SCF-MO) calculations for the energy eigenvalues of the molecular wave functions of the Ar^{12+}-Ca system. The analog correlation diagram Ar^{4+}-Ca is very much the same, just with a different ordering of the outer levels. For large internuclear distances the molecular $1\frac{1}{2}\pm$ state where $\frac{1}{2}$ denotes the projection of the total angular momentum j on the internuclear axis correlates to the Ca 1*s* state while the molecular $2\frac{1}{2}\pm$ state correlates to the Ar 1*s* state. All close-coupling calculations presented in this paper were done within the full space of the 38 molecular wave functions.

In the first step we start with the initial $Ar^{4+}(1s^2 2s^2 2p^6 3s^2 3p^2)$-Ca system and calculate the exci-

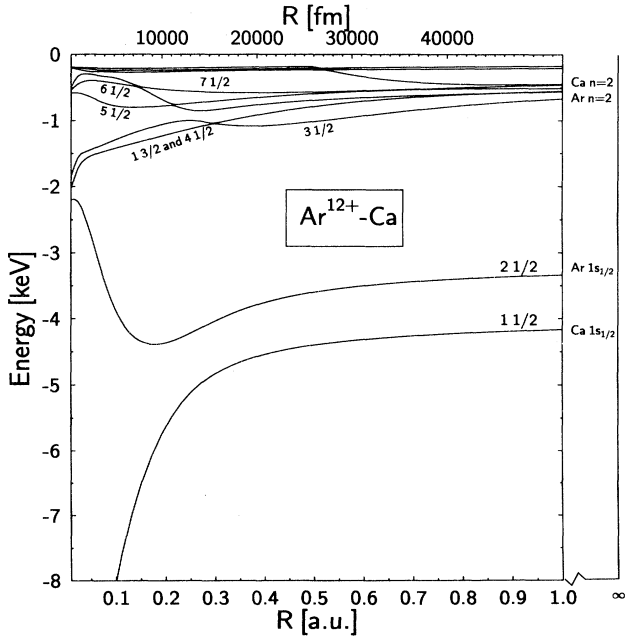

FIG. 2. Correlation diagram for the system Ar^{12+}-Ca.

tation probability for the Ar L- and Ar M-shell states in large-impact-parameter collisions. For impact parameters between 0.25 and 2.0 a.u. the mean excitation probability for both shells produced per collision ranges from 0.10 to 0.25. This impact-parameter range correlates with the principle maximum in the atomic wave functions of Ar^{4+} L- and M-shell states, which lies between 0.27 and 1.34 a.u. In a solid target with 2-$\mu g/cm^2$ target thickness which has approximately 50 atomic layers and 10-a.u. mean distance between the Ca atoms, the probability of large-impact-parameter collisions is almost unity and therefore the M and L shells of the Ar^{4+} projectile are fully ionized after a few atomic layers. The K-vacancy production rate of Ar^{4+} and Ar^{12+} in the experiment of Kambara *et al.* is therefore very much the same due to these large-impact-parameter M- and L-shell excitation and ionization processes in the Ar^{4+} projectiles. While large impact parameters are very probable, the probability for collisions with $b \leq 0.1$ a.u. is very small in thin targets. Supposing a random orientation of the Ca crystals in the target as schematically shown in Fig. 3, a simple statistical evaluation gives a probability of 5×10^{-3} to have one narrow collision with $b \leq 0.1$ a.u. in a 2-$\mu g/cm^2$ target while the probability to have two narrow collisions is 1.25×10^{-5}. From the point of view of K-L-level matching and vacancy transfer one nearly has single-collision conditions as in gas targets.

To describe the narrow collisions, where K-L-level matching occurs, we therefore start with an Ar^{12+} projectile. Comparing the atomic eigenvalues of the Ar^{12+} with those of the neutral Ca we see that the K shell of the collision partners are not swapped while the L shell of the Ar^{12+} lies below the Ca L shell. Therefore the molecular $1\frac{3}{2}\pm$ state correlates in the incoming channel to the empty Ar^{12+} $|2p_{3/2},m_j=\pm\frac{3}{2}\rangle$ state, as can be seen in Fig. 2. In a narrow collision the vacancies of the molecular $1\frac{3}{2}\pm$ state can first be shared with the $2\frac{1}{2}\pm$ state via rotational coupling and then be shared in the outgoing part of the collision between the $2\frac{1}{2}\pm$ and $1\frac{1}{2}\pm$ state via radial coupling.

From the single-particle amplitudes which we gain from solving the close-coupling equations with two initial vacancies in the doubly degenerated molecular $1\frac{3}{2}\pm$ state, we calculate the probability to find at least one vacancy in the Ar 1s (Ca 1s) state and the sum as

$$P_{\mathrm{Ar}\,1s}=|a_{1\frac{3}{2}+,2\frac{1}{2}+}|^2+|a_{1\frac{3}{2}+,2\frac{1}{2}-}|^2 +|a_{1\frac{3}{2}-,2\frac{1}{2}+}|^2+|a_{1\frac{3}{2}-,2\frac{1}{2}-}|^2 ,$$

$$P_{\mathrm{Ca}\,1s}=|a_{1\frac{3}{2}+,1\frac{1}{2}+}|^2+|a_{1\frac{3}{2}+,1\frac{1}{2}-}|^2 +|a_{1\frac{3}{2}-,1\frac{1}{2}+}|^2+|a_{1\frac{3}{2}-,1\frac{1}{2}-}|^2 ,$$

$$P_{\mathrm{sum}}=P_{\mathrm{Ar}\,1s}+P_{\mathrm{Ca}\,1s} .$$

We checked the K-vacancy probability contribution from the empty molecular orbitals $3\frac{1}{2}\pm$, $4\frac{1}{2}\pm$, and $5\frac{1}{2}\pm$ and found them to be small (≤ 0.01) in contrast to the similar collision system 10-MeV Si^{7+} on Al (solid target) where the latter three molecular orbitals show a significant contribution [20].

Figure 4 shows the impact-parameter-dependent probabilities for a Ca K-shell vacancy (full line), an Ar K-shell vacancy (dotted line), and the sum of both probabilities (chained line). Both the shape and height of the experi-

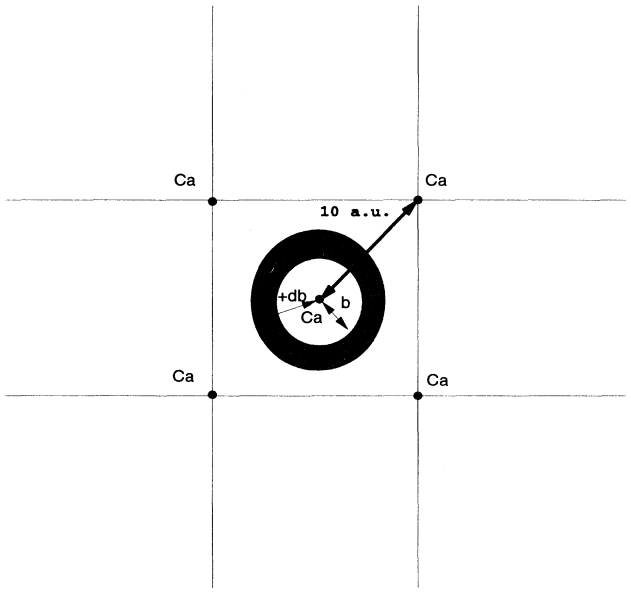

FIG. 3. Ca-target surface with a mean distance of 10 a.u. between the Ca atoms.

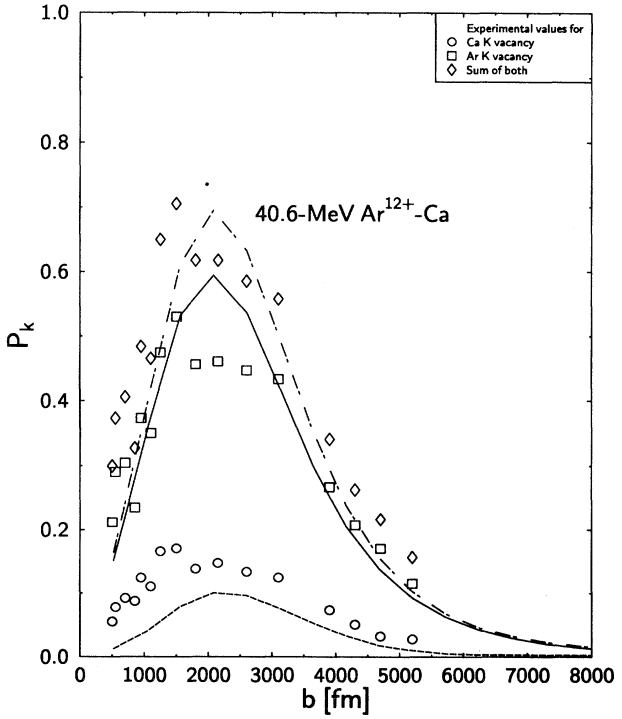

FIG. 4. Probability for Ca K-shell vacancy, Ar K-shell vacancy, and the sum of both. The experimental values are from Ref. [4].

mental values are reproduced by our 38-state calculation in a full *ab initio* way. In order to be consistent with the evaluation of the experimentalists we used the same screened Bohr potential for the nuclear trajectories as was used in the paper by Kambara *et al.* to transform the scattering angle θ to impact parameter b. Therefore the shift of the maximum in the probabilities in our calculations towards higher impact parameters can be a hint to solid-target effects in the experiment. A target thickness of 2–8 $\mu g/cm^2$ corresponds to 50–300 atomic layers, and we can expect the projectile to perform additional large-impact-parameter scattering while passing the target. These large-impact-parameter scattering processes lead to smaller effective impact parameters without raising the P_K vacancy probability.

IV. CONCLUSION

We presented *ab initio* relativistic time-dependent Dirac-Fock-Slater calculations for the *K*-*L*-vacancy-sharing process. From large-impact-parameter calculations we deduce a mean *M*- and *L*-shell excitation probability of primarily low-ionized incoming projectiles. Application to the scattering system 40.6-MeV Ar^{4+} or Ar^{12+} on Ca shows that the Ar^{4+} *M* and *L* shells are ionized while passing a few atomic layers of the Ca target and therefore Ar^{4+} acts like Ar^{12+}. For the *K*-*L*-vacancy-sharing process which takes place at small impact parameters, we start with 40.6-MeV Ar^{12+} on Ca and get both qualitatively and quantitatively good agreement with experimental results of Kambara *et al.* [4].

[1] J. S. Briggs, Rep. Prog. Phys. **39**, 217 (1976).
[2] H. Schulze, Ph.D. thesis, University of Münster, Germany, 1991.
[3] J. Eichler and U. Wille, Phys. Rev. A **11**, 1973 (1975).
[4] T. Kambara, R. Schuch, Y. Awaya, T. Mizogawa, H. Kumagai, Y. Kanai, H. Shibata, and K. Shima, Z. Phys. D **22**, 451 (1992).
[5] W.-D. Sepp, D. Kolb, W. Sengler, H. Hartung, and B. Fricke, Phys. Rev. A **33**, 3679 (1986).
[6] B. Thies, W.-D. Sepp, and B. Fricke, Phys. Lett. A **139**, 161 (1989).
[7] P. Kürpick, B. Thies, W.-D. Sepp, and B. Fricke, J. Phys. B **24**, L139 (1991).
[8] P. Kürpick, D. Heinemann, W.-D. Sepp, and B. Fricke, Z. Phys. D **22**, 407 (1991).
[9] P. Kürpick, W.-D.Sepp, and B. Fricke, Z. Phys. D **21**, S293 (1991).
[10] P. Kürpick, H.-J. Lüdde, W.-D. Sepp, and B. Fricke, Nucl. Instrum. Methods Phys. Res. Sect. B **94**, 183 (1994).
[11] P. Kürpick and H.-J. Lüdde, Comput. Phys. Commun. **75**, 127 (1993).
[12] B. H. Bransden and M. R. C. McDowell, *Charge Exchange and the Theory of Ion-Atom Collisions* (Clarendon, Oxford, 1992).
[13] J. F. Reading, Phys. Rev. A **8**, 3262 (1973).
[14] J. Reinhardt, B. Müller, W. Greiner, and G. Soff, Phys. Rev. Lett. **43**, 1307 (1979).
[15] J. F. Reading and A. L. Ford, Phys. Rev. A **21**, 124 (1980).
[16] R. L. Becker, A. L. Ford, and J. F. Reading, Phys. Rev. A **29**, 3111 (1984).
[17] H.-J. Lüdde and R. M. Dreizler, J. Phys. B **18**, 107 (1985).
[18] R. L. Becker, A. L. Ford, and J. F. Reading, Nucl. Instrum. Methods Phys. Res. Sect. **10/11**, 1 (1985).
[19] P. Kürpick, H.-J. Lüdde, W.-D. Sepp, and B. Fricke, Z. Phys. D **25**, 17 (1992).
[20] P. Kürpick, W.-D. Sepp, and B. Fricke (unpublished).